International Journal for Multidisciplinary Research (IJFMR)
E-ISSN: 2582-2160 ● Website: www.ijfmr.com ● Email: editor@ijfmr.com

The Transfer Function Characterization and Linearization Using an Inductive Coupling Circuit for System Measurement in Hard-To-Reach Location and in Medical Diagnostics

Abdulwahab Deji[1], Sheroz Khan[2], Musse Mohamud Ahamad[3]

[1]Department of Electrical Computer Information and Telecommunication Engineering, Waidsum University Malaysia.
[2]Department of Electrical Engineering, Faculty of Engineering, Onaizah College, Saudi Arabia.
[3]Department of Electrical and Computer Engineering, Faculty of Engineering, University of Malaysia Sarawak.

Abstract
This research paper demonstrates the scope and potential of a circuit design of the differential sensory system, functional theory and relevant derivations on its operation details when characterizing their transfer function for signal gain. The idea is using inductive coils as transducer elements responding to changes in the parameter being sensed. This phenomenon is the result of simple movement of a core position bringing about proportionate changes in the inductance of the circuit, and hence ultimately in the output parameters. The output parameters include frequency, duty cycle, current, voltage, frequency, frequency hysteresis, speed, acceleration, kinematics, pressure, range of oscillation, angulation, Impedance voltage, Magnetic field strength, and Transfer function. The results shown can be used for characterizing the materials and hence sensor with high sensitivity, linearity and responsiveness in harsh environmental condition is obtained and characterized and their corresponding transfer functions are obtained. This help in sensing broken metallic in the body during war and sensed in hard to reach to reach locations as a result of the huge magnetic field generated. This also, verifies the derivations and the simulation in literature.

Keywords: Frequency, Duty Cycle, Current, Voltage, Frequency, Frequency Hysteresis, Speed, Acceleration, Kinematics, Pressure, Range of Oscillation, Angulation, Impedance Voltage, Magnetic Field Strength, And Transfer Function, excitation voltage, excitation current

1. Introduction

The transfer function seeming characteristics for determining the performance of the system under consideration or the response of the designed system in both time domain and in frequency domain. This transfer function is sub-sectioned into output transfer characterization with the impedance voltage, input transfer characterization with the impedance/sensing voltage and the transfer function with the excited current. [Khan S., Deji A., Zahirul A.H.M., Chebil J., Shobani M.M., Noreha A.M. Setember 2012)], [Deji A., Sheroz K, Musse M.A, Jalel C. (August 2014)]. These characteristics, (transfer function or

system function or network function) of an engineering system, or sub-system, or component is a mathematical derivative function that models a given design's output for each possible input parameter. In different research papers, different input and output parameter are modelled and their transfer functions or system function can be obtained (Deji A., Sheroz K., Musse M.A 2014). Transfer function can be obtained from different instrumentation and control engineering. In this case this paper reference the inductive sensing transfer function. Nowadays, these sensors transfer characteristics are popularly used in the automatic industry and laboratory experiments, especially in the area of biomedical and biotechnology engineering, communication engineering, oil and gas engineering, drilling and geology/geophysics and petroleum engineering to measure many different physical parameters, such as force, pressure and position. Civil engineers have the ability to measure rebar corrosion, structural defects and cracks with the help of this type of improved sensors. (Deji A., Sheroz K., Jalal C., Zahirul A.M.H. 2011). The Transfer Function of a circuit is seen as the ratio of the output signal to the input signal in the frequency domain, and it applies only to linear time-invariant systems (E.E Practical). It is a key descriptor of a circuit, and for a complex circuit the overall transfer function can be relatively determined from the transfer functions of its subcircuits or subsystems. Transfer functions are typically denoted with H(s) (Deji A., Sheroz K., Musse M.A 2012). In electrical circuit system, signals are usually voltage or current. A circuit's input signal may be current or voltage and its output could be either same parameter as well. This creates four types of transfer functions as shown in table 1. Deji A., Sheroz K, Musse M.A, Jalel C. (2011)

Table 1: Transfer Function types and Characteristics (Practical EE Copyright 2019)

Transfer Type	Output / Input	Units
Transadmittance H(s)	I(s) / V(s)	1/Ω
Voltage H(s)	V(s) / V(s)	Unitless
Current H(s)	I(s) / I(s)	Unitless
Transimpedance H(s)	V(s) / I(s)	Ω

In this paper, the modelling of the transfer function characterization is based on differential Inductive system for measurement in hard-to-reach location especially in power system and electromagnetic system. The system model is shown in figure 1.

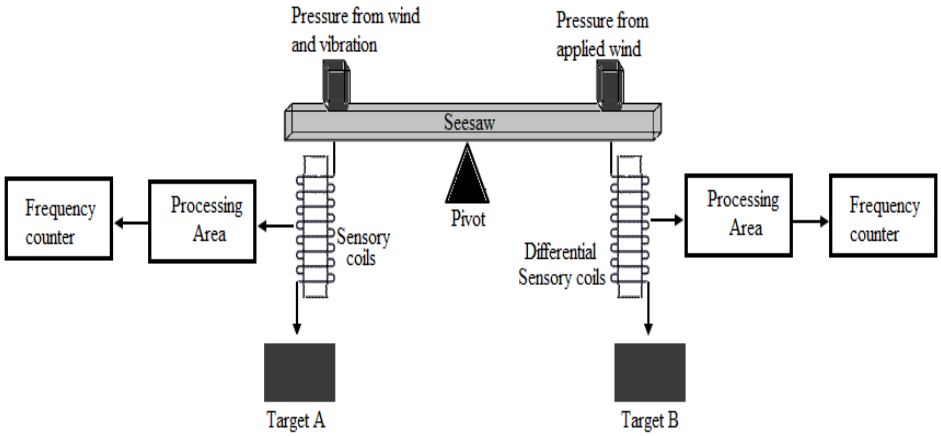

Figure 1: New sensor model for measurement

2. Analytical Model

In this section, the transfer function model is proposed and the conceptual structural design of the novel displacement sensor characterization and it transfer function from magnetic field and voltage generated on its working modules mechanism is schematically shown in Figure 1. The variation in the physical parameter such as (force or pressure) cause equivalent changes the inductance of the coil connected to an interface circuit (555 timer-based), which converts this deviation into useful frequency output, voltage, Magnetic field and Transfer functions. (Deji A., Sheroz K., Mohammed H.H,. November 2023). Here it shows how the novel displacement deviation sensor works in transforming changes in inductance into proportionate frequency and voltage output and transfer function characterization and Linearization is presented. [Deji, A., Khan, S., Habaebi, H.M., Musa. O.S. (2024)], [Deji A., , Sheroz K., Musse M.A., (Jan-Feb 2024)], [Deji A., Sheroz K., Musse M.A., (December 2023)]

2.1 Series and Parallel Combinations

If two subcircuits are connected in series, then the overall transfer function is the product of the transfer functions of the subcircuits. If two subcircuits are connected in parallel, and their outputs are summed, then the overall transfer function is the sum of the transfer functions of the subcircuits.

2.1.1 Series Connection of Transfer Functions

The transfer function modelling is shown in the series circuit below;

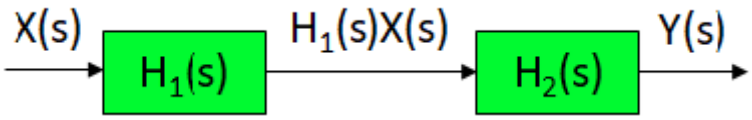

Figure 1: Series Connection of Transfer Function

$$H(s) = \frac{Y(s)}{X(s)} = H_1(s) \cdot H_2(s) \quad (1)$$

2.1.2 Parallel Connection of Transfer Functions

The parallel connection of a transfer function characteristics is shown in figure 2 below.

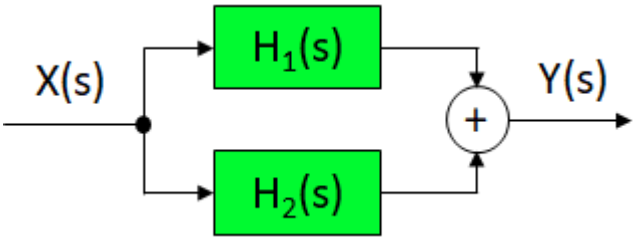

Figure 2: Parallel Connection of Transfer Functions

$$H(s) = \frac{Y(s)}{X(s)} = H_1(s) + H_2(s) \quad (2)$$

A circuit that has two subcircuits in parallel with a 3rd subcircuit, the overall transfer function is modelled below;

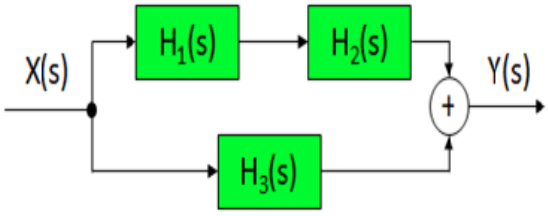

Figure 3: Determine Overall Transfer Function

The series elements multiply to make: $H_1(s) * H_2(s)$. This is then in parallel with $H_3(s)$. So, the overall transfer function is:

$H(s) = Y(s) / X(s) = H_1(s) * H_2(s) + H_3(s)$ (3)

2.1.3 Feedback Transfer Function

The diagram below shows a feedback control system with G(s) forward gain, and H(s) feedback transfer function. E(s) is the error signal, which is the difference between the input signal X(s) and the feedback signal H(s)Y(s).

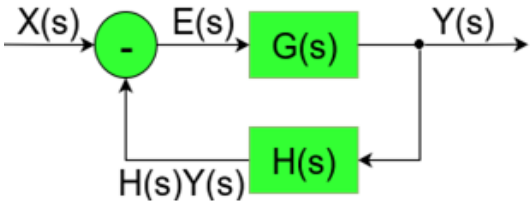

Figure 4: Feedback Control System

$$E(s) = X(s) - H(s) \cdot Y(s) \quad (4)$$

$$Y(s) = G(s) \cdot E(s) \quad (5)$$

The overall transfer function of a feedback system, which is sometimes called the closed-loop transfer function, is the [forward gain] / (1 + [open-loop gain]) (Practical EE Copyright 2019)

This research paper model the magnetic field, current and voltage transfer functions for characterizing measurement and feedback in hard-to-reach location for electrical energy and power systems applications

2.2 Magnetic Field, Current and Voltage from The Differential Position Of The Sensory System

The relationship between excitation magnetic field and excitation current provided by the input voltage V_{CC} is given as: [Deji A., Sheroz K, Musse M.A, Jalel C. (2011)], [Abdulwahab Deji (2016)]

$$B_{exc} = \frac{K_B \mu_0 \mu_r N^2 I_{exc} A}{l} \quad (6)$$

Where K_B is the seesaw constant and it's 64.

The excitation current produced in the system is given as:

$$I_{exc} = \frac{-V_{exc}}{R_s // R_1 + R_2 + R_3} \quad (7)$$

The total resistances in series arrangement is given as:

$$R_T = R_1 + R_2 + R_3 \quad (8)$$

The excitation current has been reduced to;

$$I_{exc} = \frac{-V_{exc}}{R_S // R_T} \quad (9)$$

Where V_{exc} is the input sinusoidal voltage of the excitation circuit with amplitude A_{exc} and frequency $f_{exc.}$ The readout is a standard 555 timer connected to a low noise instrumentation conditioning driven by sinusoidal voltage V_{timer} with amplitude A_{timer} and frequency $f_{timer.}$

The sinus wave $V_{LR(t)}$ across the resonant circuit with excitation current I_{exc} produced by V_{cc} in the timer circuit is given as:

$$V_{RL(t)} = R_S // R_T \times I_{exc} Sin(2\pi f_R * t) \quad (10)$$

The target Resistance of measurement is given as:

$$R_D = R_S // R_T \quad (11)$$

$$V_{RL(t)} = R_D \times I_{exc} Sin(2\pi f_R * t) \quad (12)$$

Where R_S is the resistance from the sensing target, R_T is the total sensing resistance and R_D is sum of the target resistance parallel to the position sensing resistances.

The voltage output as a result of the sensing electrode of the inward coil geometry is given as:

$$V_{OUT(inward)} = I_{exc} * \frac{\mu_0 N^2 A}{l}(1 + \frac{x}{l}(\mu_r - 1)) \quad (13)$$

While the voltage output as a result of the sensing electrode of the outward coil geometry is also given as:

$$V_{OUT(outward)} = I_{exc} * \frac{\mu_0 N^2 A}{l}(\mu_r + \frac{x}{l}(1 - \mu_r)) \quad (14)$$

The response readout or the transfer function of the inward core geometry from the instrumentation electronics is given as:

$$\frac{V_{OUT(INWARD)}}{V_{TIMER}}(s) = \frac{V_{OUT(inward)} = I_{exc} * \frac{\mu_0 N^2 A}{l}(1 + \frac{x}{l}(\mu_r - 1))}{R_S // R_T \times I_{exc} Sin(2\pi f_R * t} \quad (15)$$

Therefore, the transfer function for inward magnetic core movement is:

$$H = \frac{V_{OUT(INWARD)}}{V_{TIMER}}(s) = (s)\frac{\frac{\mu_0 N^2 A}{l}(1 + \frac{x}{l}(\mu_r - 1))}{R_S // R_T \times Sin(2\pi f_R * t)} \quad (16)$$

The response readout or the transfer function of the outward core geometry from the instrumentation electronics is also given as:

$$\frac{V_{OUT(OUTWARD)}}{V_{TIMER}}(s) = \frac{V_{OUT(OUTWARD)}}{V_{TIMER}} = \frac{I_{exc} * \frac{\mu_0 N^2 A}{l}(\mu_r + \frac{x}{l}(1 - \mu_r))}{R_S // R_T \times I_{exc} Sin(2\pi f_R * t} \quad (17)$$

Therefore, the transfer function for inward magnetic core movement is:

$$H = \frac{V_{OUT(INWARD)}}{V_{TIMER}}(s) = (s)\frac{\frac{\mu_0 N^2 A}{l}(\mu_r + \frac{x}{l}(1 - \mu_r))}{R_S // R_T \times Sin(2\pi f_R * t)} \quad (18)$$

2.3 Angular Displacement of Core from the Position Sensor.

Angular displacement is seen as the angle in radians through which a point has been rotated about a specified axis. It is the distance an object moves in a curved path. It is represented by the length of the arc of curved path. Its unit is angle. It is shown in Figure 6.

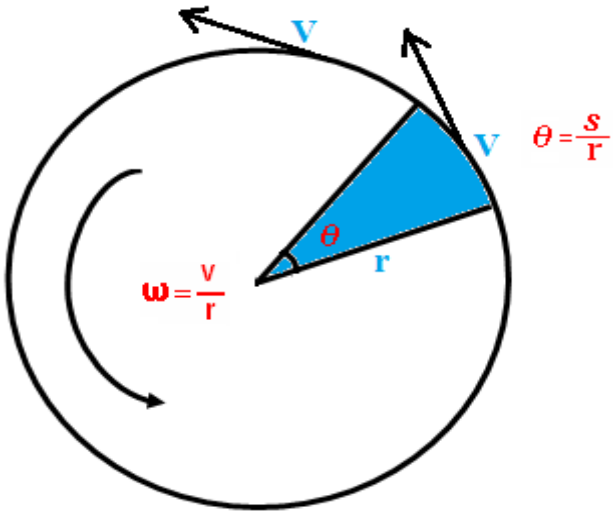

Figure 6: Angular Displacement due to Core misalignment.

From Figure 6, the length of the arc x, is given as;

$$x = \frac{\theta}{2\pi} \times 2\pi r = r\theta \qquad (19)$$

The angular displacement is given in equation (20)

$$\theta = \frac{x}{r} \qquad (20)$$

Substituting equation 19 into our previous equation of inductance, then will obtain the output inductance as a function of the angular displacement, thereby causing misalignment of the core inward movement. Hence; [Deji A., Sherifah OM., (2023], [Elfaki Ahamed, O.M.H., Musa O.S, Deji A., 2023]

$$L_{\theta IN} = \frac{\mu_0 N^2 A}{l}\left(1 + \frac{r\theta}{l}(\mu_r - 1)\right)$$

$$L_{\theta IN} = \frac{\mu_0 N^2 A}{l}\left(\frac{l + r\theta}{l}(\mu_r - 1)\right)$$

$$L_{\theta IN} = \frac{\mu_0 N^2 A}{l^2}(l + r\theta(\mu_r - 1)) \qquad (21)$$

Again, substituting equation 20 into our previous equation of inductance, then will obtain the output inductance as a function of the angular displacement, thereby causing misalignment of the core outward movement. (Deji A., Sheroz K., Musse M.A., November 2023).

$$L_{\theta OUT} = \frac{\mu_0 N^2 A}{l}\left(\mu_r + \frac{r\theta}{l}(1 - \mu_r)\right)$$

$$L_{\theta OUT} = \frac{\mu_0 N^2 A}{l}\left(\frac{\mu_r l + r\theta}{l}(1 - \mu_r)\right)$$

$$L_{\theta OUT} = \frac{\mu_0 N^2 A}{l^2}(\mu_r l + r\theta(1 - \mu_r)) \qquad (22)$$

Substituting our previous pressure equation into our previous equation of inductance, we had the angular displacement as a function of differentially applied pressure. (Deji A., Sheroz K., Musse M.A., November 2023)

$$\theta = \frac{x}{r} = \frac{\frac{(P - P_{wind})At^2}{2m}}{r}$$

$$\theta = \frac{x}{r} = \frac{(P - P_{wind})At^2}{2mr} \quad (23)$$

Again, our previous inductance equation into our previous equation of frequency, we will obtain the frequency output as a function of the inductance resulting from misaligned angular inward displacement. This is shown as: (Deji A., Sheroz K., Musse M.A., November 2023)

$$f_{\theta IN} = \frac{1.58R}{\frac{\mu_0 N^2 A}{l^2}(l + r\theta(\mu_r - 1))}$$

$$f_{\theta IN} = \frac{1.58Rl^2}{\mu_0 N^2 A(l + r\theta(\mu_r - 1))} \quad (24)$$

Also, substituting our previous inductance equation into our previous equation of frequency, we will obtain the frequency output as a function of the inductance resulting from misaligned angular outward displacement. This is shown as:

$$f_{\theta OUT} = \frac{1.58R}{\frac{\mu_0 N^2 A}{l^2}(\mu_r l + r\theta(1 - \mu_r))}$$

$$f_{\theta OUT} = \frac{1.58Rl^2}{\mu_0 N^2 A(\mu_r l + r\theta(1 - \mu_r))} \quad (25)$$

From equation 20, we obtain the first derivative of the angular displacement, which gives the angular velocity of the motion of the core into and out of the coils geometry. This is shown as:

$$\frac{d(x)}{dt} = r\frac{d(\theta)}{dt} = r\omega = v \quad (26)$$

The second derivative of the transfer function is shown in equation 27

$$\frac{d(v)}{dt} = \frac{d^2(x)}{dt^2} = r\frac{d^2(\theta)}{dt^2} = r\frac{d(\omega)}{dt} = \alpha \quad (27)$$

The RC based timer arrangement for the capacitive sensing is shown in Figure 7

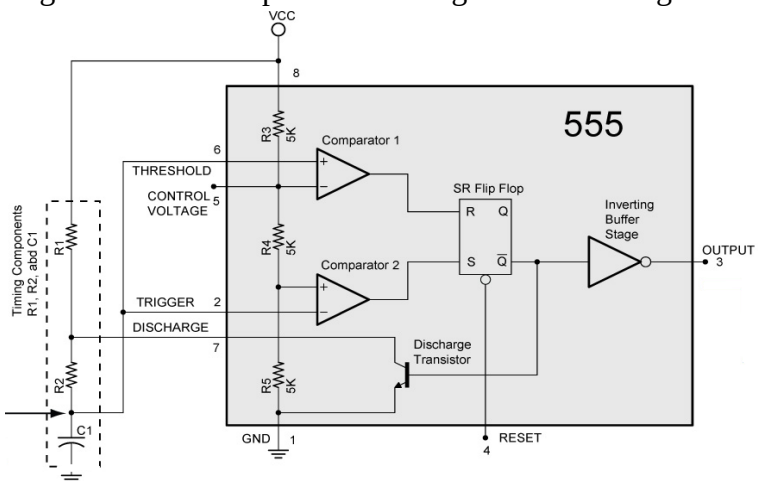

Figure 7: RC-Timer circuit configuration. Deji A., Sheroz K, Musse M.A, Jalel C. (2011)

This section discusses the analytical derivation result of differential inductance transducer measurement circuit. As earlier shown in Figure1, when the core is moving upward, a displacement is caused by force over an area in the coil and it's donated by x. Conversely, when the core is moving downward, x is calculated by displacement of core in coil. A Matlab tool is used to obtain this derivation. When L_1 is increased, x is increased also. Meanwhile, when L_2 is decreases, x increases. The frequency of L_1 is decreased exponentially and frequency of L_2 is increased exponentially as displacement is increased. Thus, the inductance is increased when displacement of air is decreased and displacement of core in coil is increased. From derivation above, we can see that at the equilibrium position, inductance of L_1 and L_2 are identical. Deji A., Sheroz K., Musse M.A., (December 2023)], [Deji A., Hanifah A.M., Sherifah O.M., (December 2023

3. Simulation Characteristic Linearization Using Diode

The diode in conjunction with the resistors gives the desired characteristic linearization and an improved model design.

4. 3.1 R_1LR_2 circuit with diodes for Left arm of sensor for characteristic linearization

The circuit configurations for the left arm is shown in Figure 9 are simulated using PSpice to observe the process of magnetization and demagnetization of the inductor as well as charging and discharging of the capacitor are shown in Figure 10. This shows the result of the simulation when using Rl3R configuration (Ezzat 2011), (Deji A, Sheroz K., Musse M.A.,2012, 2013, 2014.)

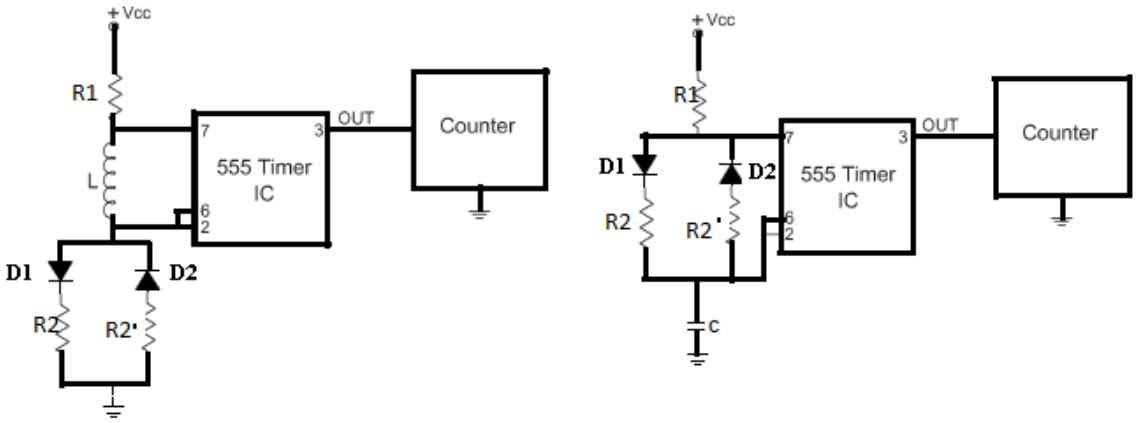

Figure 9: RL3R circuit for left arm linearization

In the circuit of Figure 9, the inductor is getting magnetized throw R_1 and R_2, when the voltage across R_2 reaches 2/3 Vcc. The coil begins to demagnetize throw R_2. Figure 10 shows the waveform for this circuit. The output voltage is the red line, while the blue line is the R_2 current with values from 2 to 5 mA. The green line is the R_2' current with values from -10 to 10 nA which is very small compared to R_2 current. So by neglecting R_2' current, we can say that the coil get magnetized throw R_1 and R_2 and demagnetized throw R_2 only.

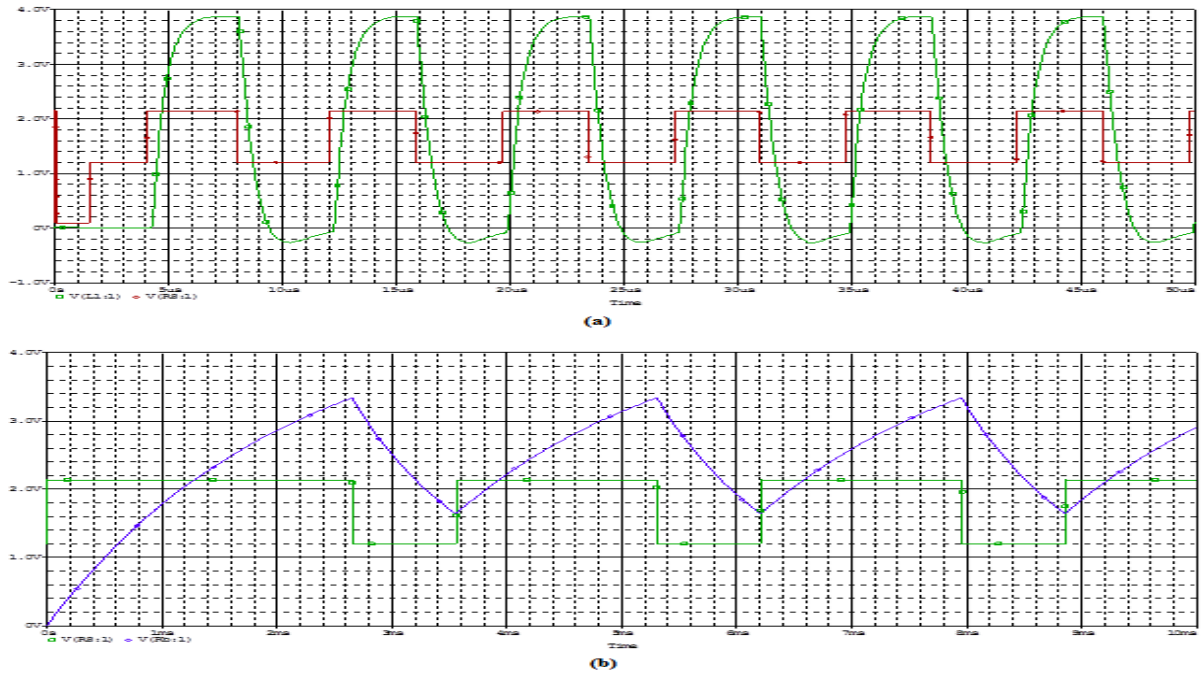

Figure1: Simulation of the position sensor circuit with diode for linearization

The frequency output from the charging and discharging concept with respect to the duty cycle is:

$$f = \frac{1}{L_{wind}\left(1+\frac{x}{l}(\mu_r - 1)\right)\left[\frac{0.693}{R_2} + \frac{1}{R_1+R_2} In\left(\frac{2R_1 - R_2}{R_1 - 2R_2}\right)\right]} \quad (28)$$

$$f = \frac{1.44}{C(R_1 + 2R_2)} \quad (29)$$

The plot for the frequency variation with respect to the displacement *x* is shown in Figure 11. Only the plot from the right arm coil is presented here. Although the variation of frequency is affected by the variation of displacement and its applicable to both inductors and capacitors. The search is focused more towards the inductive sweeping and changes. It can be seen that the frequency keeps on decreasing as the displacement *x* of core insertion into the coil is increasing (Ezzat 2011),), (Deji A, Sheroz K., Musse M.A.,2012, 2013, 2014 and 2023)

.

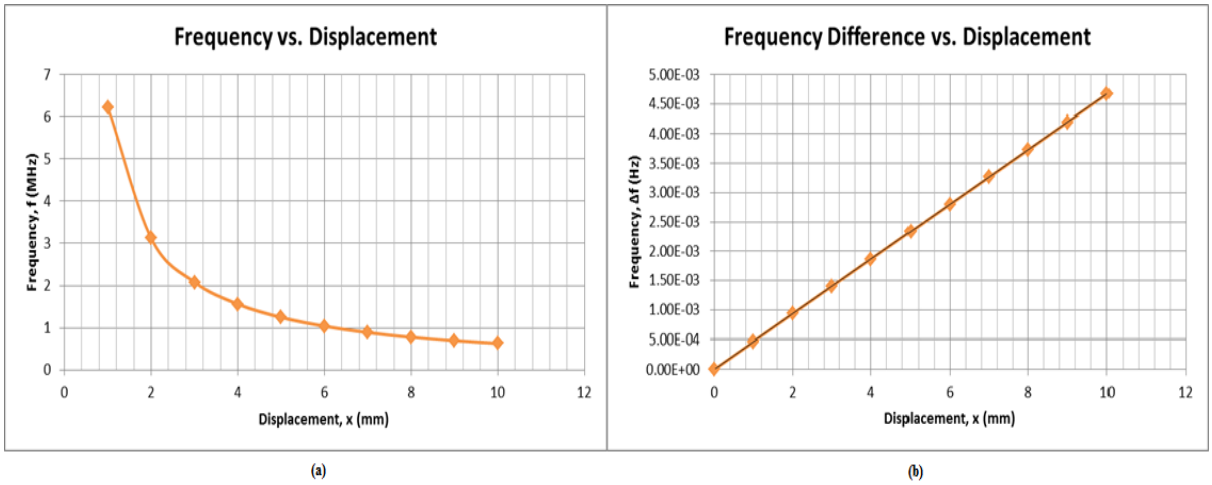

Figure 11: (a) frequency with displacement, (b) Variation of differential frequency with displacement.

From this research, it is discovered that the IC 555 timer has various application. It can be used as a normal timer, or it's used as an oscillator in a circuit that converts the unknown capacitance and inductance to frequency variations. The duty cycle is given by [Abdulwahab D. et al., (2010)], [Abdulwahab D., S. Khan, Chebil J., and Alam A. H. M. Z., (2011)],

$$\% DC = \frac{t_H}{t_H + t_L} = \frac{t_H}{T} \% \qquad (30)$$

By adding the diodes in the circuit configuration, as in Figure 7, the duty cycle of the circuit are improved, where the difference between R_1 and R_2, as well as $R_{2'}$, are relatively low, hence reducing the linearity issue. Moreover, the sensitivity of the sensor is also increased.

From the derivations and plots above, it can be seen that the movement of the core, either into or out of the coil, is responsible for the variations of frequency and the frequency difference. The variation of frequency difference with respect to the depth, i.e. displacement *x*, is observed through the plots obtained. Based on the derivation and plots obtained, it can be said that the frequency difference in the circuits are the same. For the circuit configuration of Figure 7, the plot of frequency difference is shown in Figure 8 and is linear. A similar plot is obtained for the frequency difference of the circuit configuration. This shows how sensitive the system is when the cores are inserted or pulled out from the coil at the same time. The current and voltage transfer functions from magnetization and demagnetization are simulated as shown in Figure 12

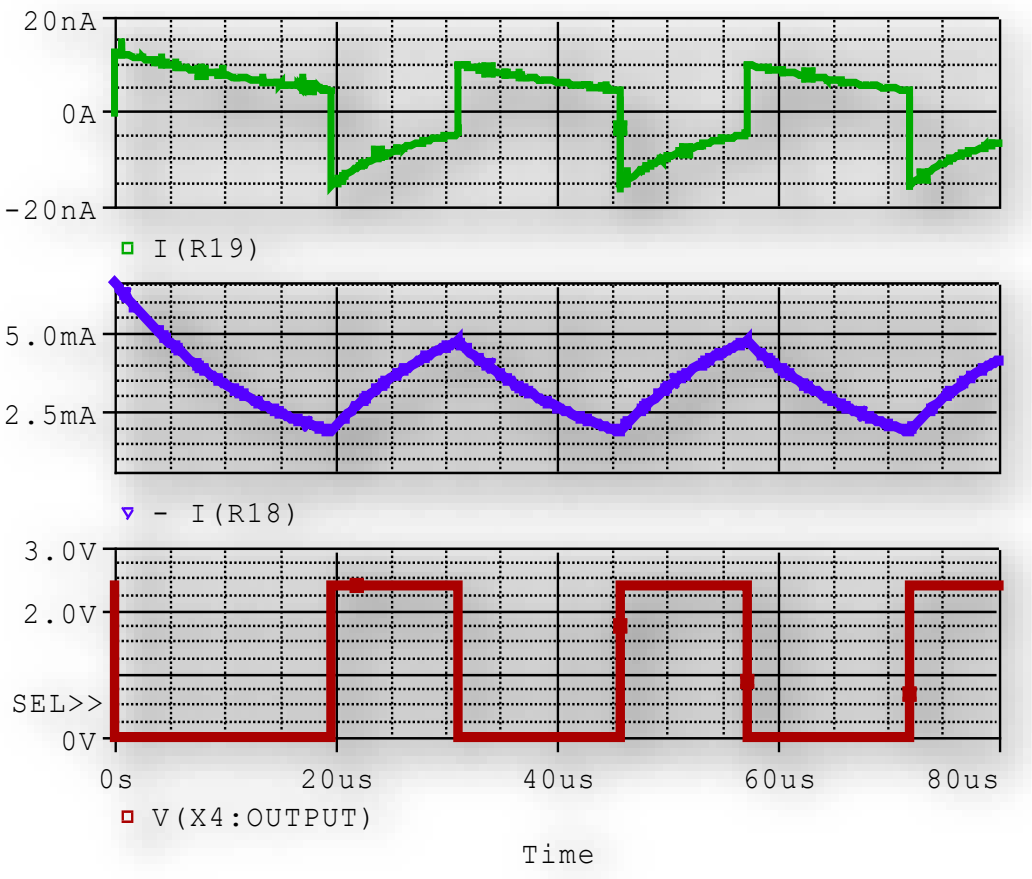

Figure 12: Current and voltage waveform for magnetization and demagnetization

5. 3.2 R_1R_2C circuit with diodes for circuit Linearization

This circuit shows a capacitor charging throw R_1 and R_2. When the voltage across the capacitor reaches 2/3 Vcc, it begins to discharge through R_2'. Figure 13 shows the simulation result of the circuit that describes the output voltage and the Capacitor voltage as shown in Figure 13.

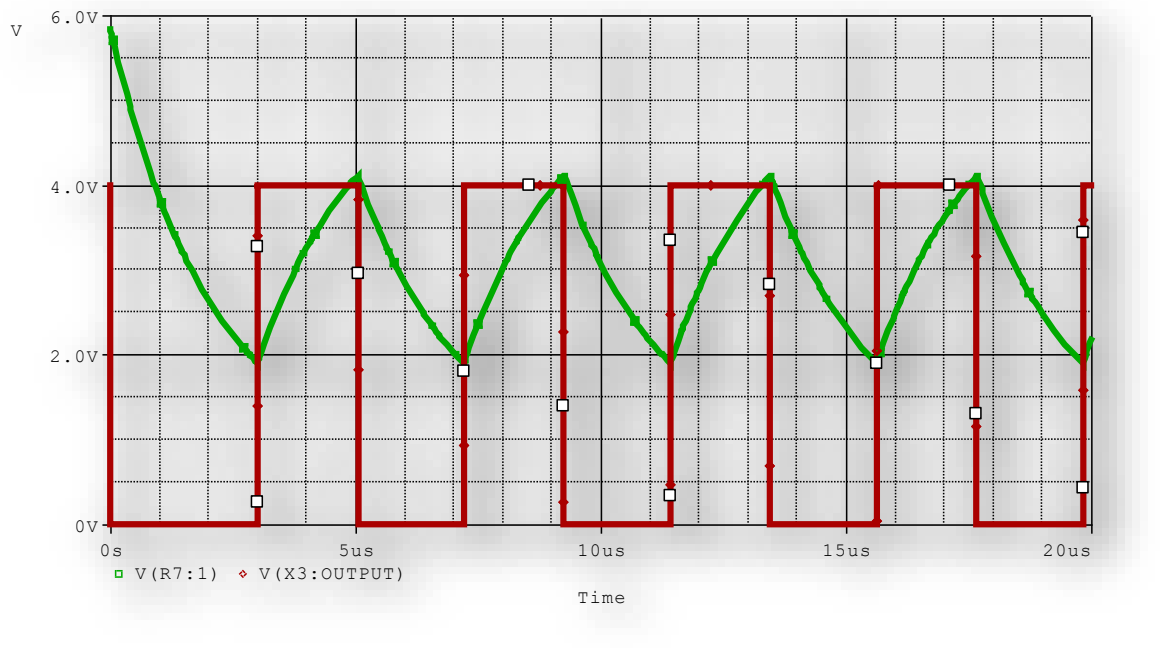

Figure 13: The output voltage and the capacitive voltage

6. Simulation of Resonant Frequency of the Designed Differential Position Sensor

The differential position sensor performs incredibly at resonant frequency. This gives room for the circuit applicability in the area of the target mass and the mass of the bar in the hard-to-reach locations. The simulation of the developed sensor is shown in the subsections below.

7. 4.1 The effect of Resonant Frequency with target mass, excitation current and magnetic Field Functions.

The mass of the bar together with the mass of the target object to be sensed are harnessed and the value are obtained, simulated and recorded. The resonant frequency is obtained in the analytical modeling presented previously. At this resonant frequency, the target can be sensed and processed. At this point, the inductance enables the position sensor to sense the designated mass of the target and bar. The sensed mass of the target and bar is plotted against the resonant frequency. In this result the resonant frequency is higher than the sensed mass. This enables the circuit to sense the parameter of interest. This result is shown in Figure 14.

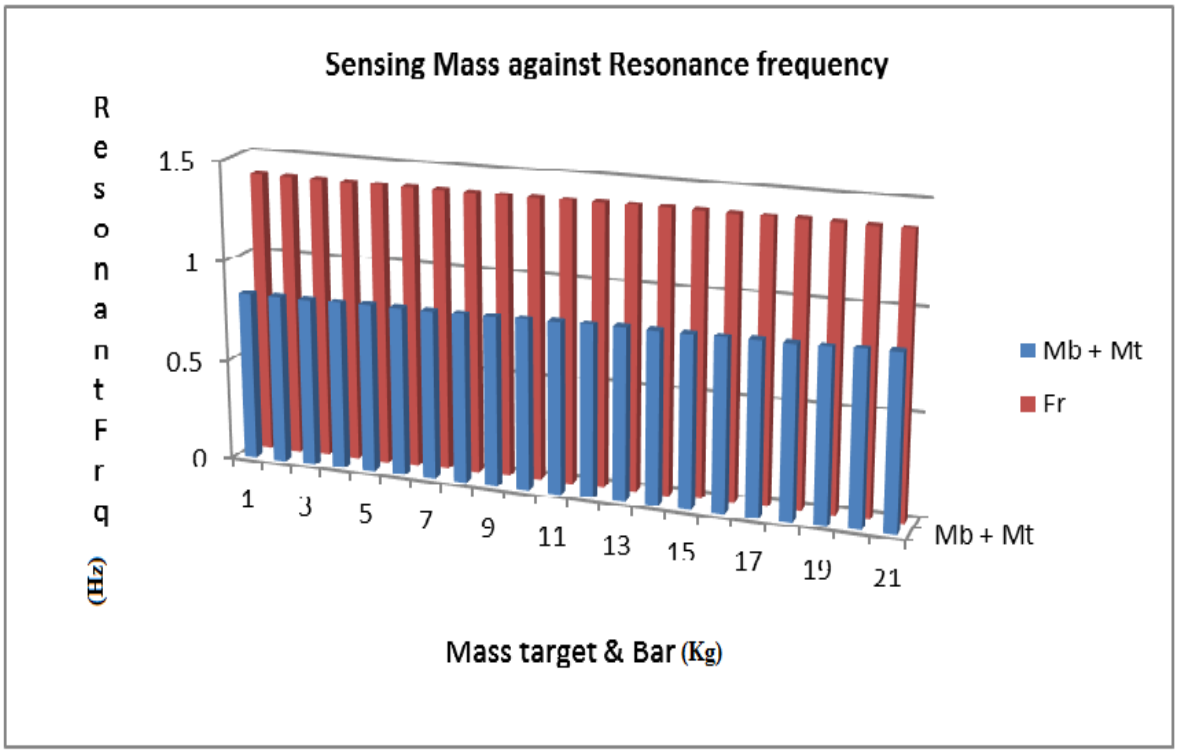

Figure 14: Resonant Frequency against target and bar mass

However, when the resonant frequency is plotted against the excitation current, the current becomes far higher than the resonant frequency. This current becomes linearly proportional to the input parameter bringing about the state of resonance. This result is shown in Figure 15

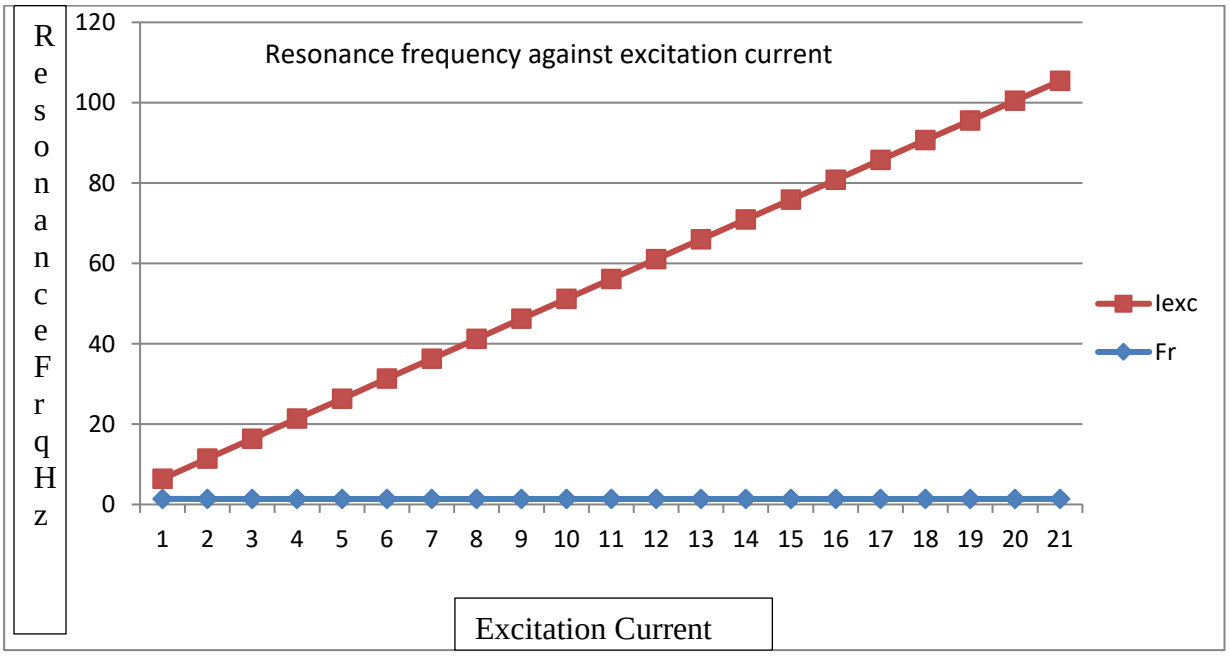

Figure 15: The resonance frequency against the excitation current

The resonant frequency is again plotted with the magnetic field strength. The magnetic field increases in a similar way as the excitation current. The resonant frequency reached is constant at this point with a low

value. The field increases as the sensing continues giving rise to a high magetic field value as shown in Figure 16. This magnetic field increases as the core goes in from the right arm of the position sensor with oscillatory mechanism and also decreases as the core goes out from the left arm of the convulsion bar with the resonant frequency remaining constant and small when compared to the value of the field generated around the coil. This help in sensing metallic objects, usually those deposited into our body during the wars, natural disaster, like flood, earthquake, Tsunami, Tonadoes etc. This sensed parameter is determined by the amount of voltage, frequency, current generated at the output counter. Since, it's a transducer, its function is to detect/sense objects, processes them using an oscillator (in this case, the 555 timer is applied as an oscillator) and this gives result at the counter for storage, for analysis and other applications such as archiving. The amount of the field generated determines to what extent the transducer can sense in the hard to reach objects. The magnetic field and the resonant frequency relationship is shown in Figure 16.

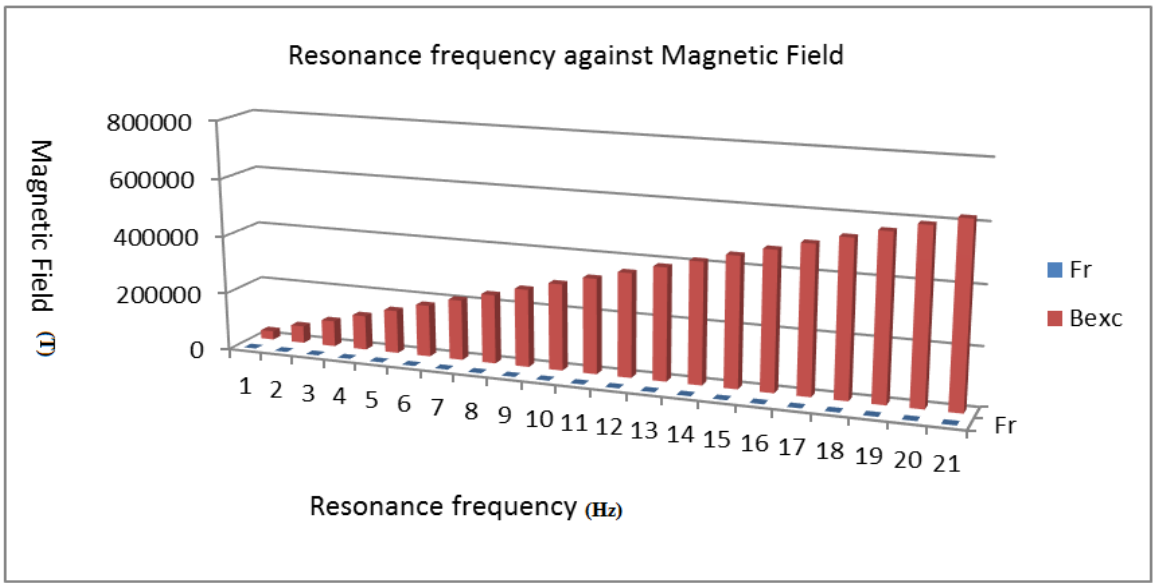

Figure 16: The effect of the Resonance frequency on the magnetic field

7.2 The Effect of the Excitation Current, Magnetic Field and the Sensing Voltage Function

Again, the magnetic field generated at this junction is compared with the excited current produced from the processor (555 timer). Since, the Vcc is applied to a part of the transducer (although not the sensing area), it initiates current to flow in the transduction. This current obtained, creates the magnetic field in the region in space around the coils. At this point, the core experiences a force which result to the magnetic field produced. The field is graphed with the amount of current flowing at this point in the sensing area. The graph shows that the current is the same in the transduction while the field increases linearly due to other parametric, probabilistic, stochastic parameters that have been assumed in the simulation. This shows that the field generated is huge at the expense of the current flowing as shown in Figure 17. All of these, shows clear cut value of the differentially designed position sensor.

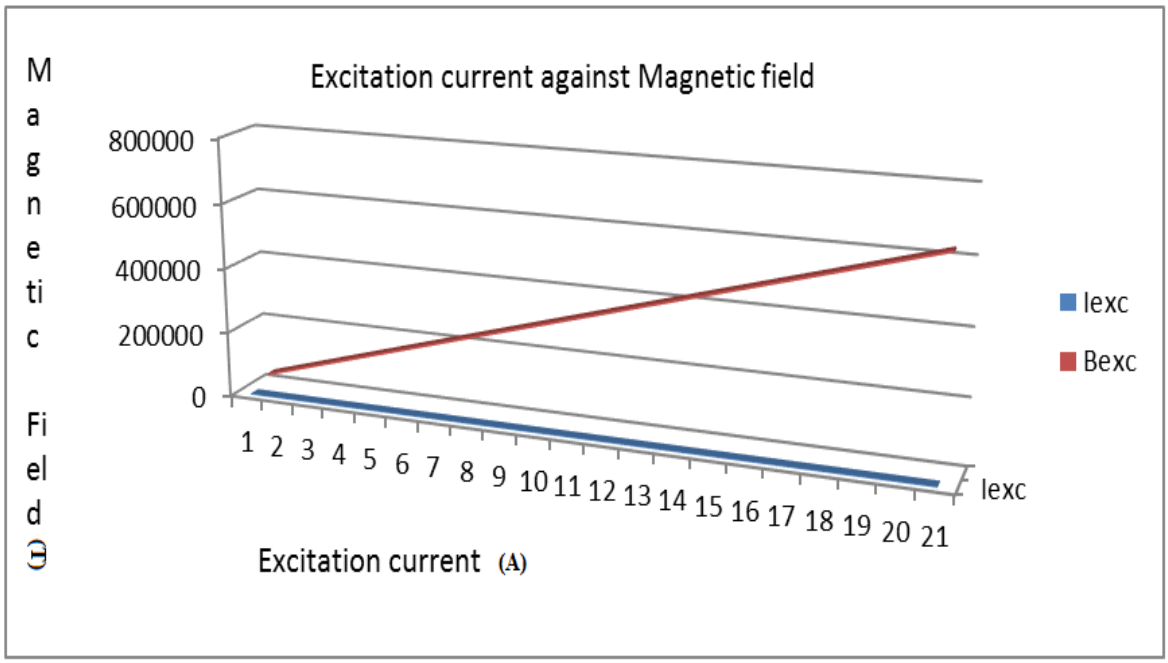

Figure 17: The effect of the excited current on the magnetic field

Furthermore, the voltage at the output of the sensor (not the Vcc) as a result of the excited current which is ultimimately a function of the impedance from the transduction ($V_{LR(t)}$), is compared with the current exciting the change. This voltage is exponential as expected owing to the fact that the resultant effect of the impedance of the inductor and resistor. Figure 18 shows the relationship between this voltage and the excited current. It is observed, that the current increases linearly due to oscillation, while the impedance voltage experiences an exponential increment giving rise to the fact both the inductance and resistance play significant role in the sensing part in particular and in the whole transduction functionality in general. The eminent impedance voltage is helpful in obtaining the transfer function of the position transducer as shown in section 5. The applied transducer gave a result of this magnitude.

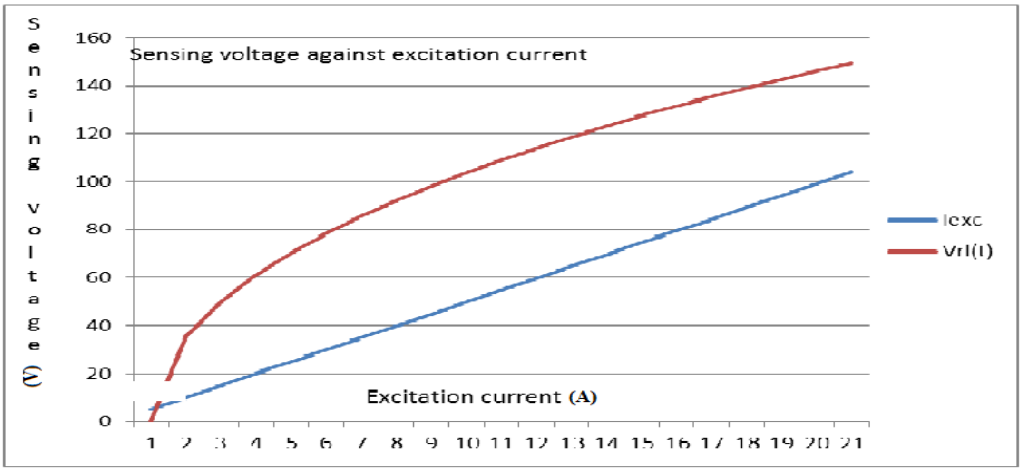

Figure 18: The effect of the excited current on the impedance voltage Function.

In another scelerio, looking at the magnetic field and the impedance voltage was not too far fetched. The graph in Figure 19 shows a clear cut in the sense that the magnetic field values generated are way higher than the impedance voltage as expected. The magnetic field increases linearly with large values as

compared to the impedance or sensing voltage. This impedance voltage ($V_{LR(t)}$), at this point remain insignificant when comparing it with the value added with magnetic field since this is the region in space the coils experiences a force, hence generating these field from both arm of the oscillatory position sensor. The impedance voltage output has small values as seen in Figure 18 while the magnetic field has an output large enough to enable the designed position transducer to sense any hidden parameter in human body or in a hard to reach location.

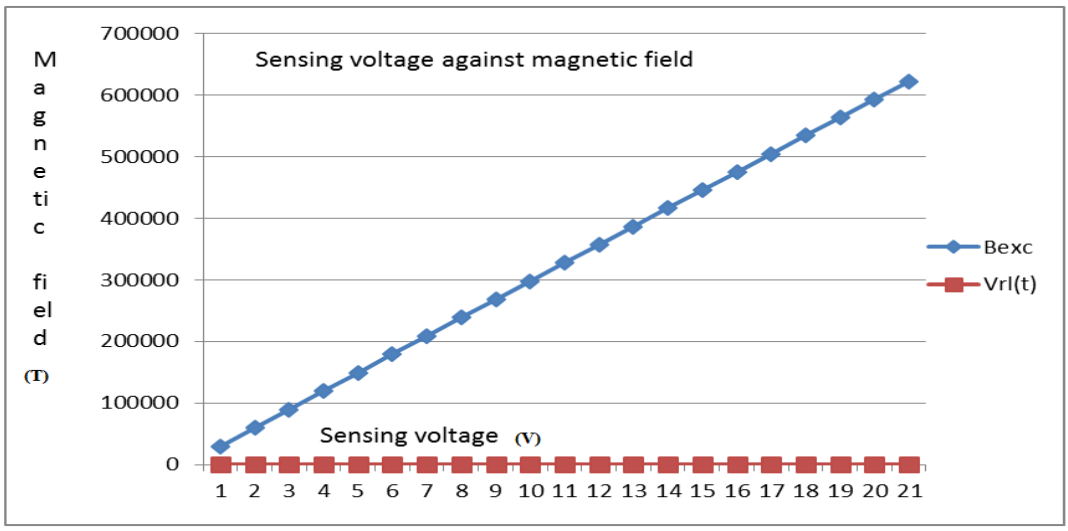

Figure 19: The effect of the magnetic field on the impedance voltage Function

7.3 Pressure and Temperature Variation with Air Density Functions

From Figure 20 (a), the contribution of the air or wind pressure is seen to have a smallest effect on the seesaw oscillation, while the pressure from the force acting on an area and hence pressure difference have both substantially contributed immensely to the seesaw oscillation. At this point, the air density was varied at different temperature thereby providing the characteristic effect in Figure. 20 (a) and (b). The pressure difference and the core pressure increase as the air density increases. This shows that at higher the temperature, density is higher and hence the pressure produced is greater causing more oscillation which indicates more parameter being sensed and ultimately producing a larger amount of frequency signal in the output pin 3 which is then fed to the counter for further usage.

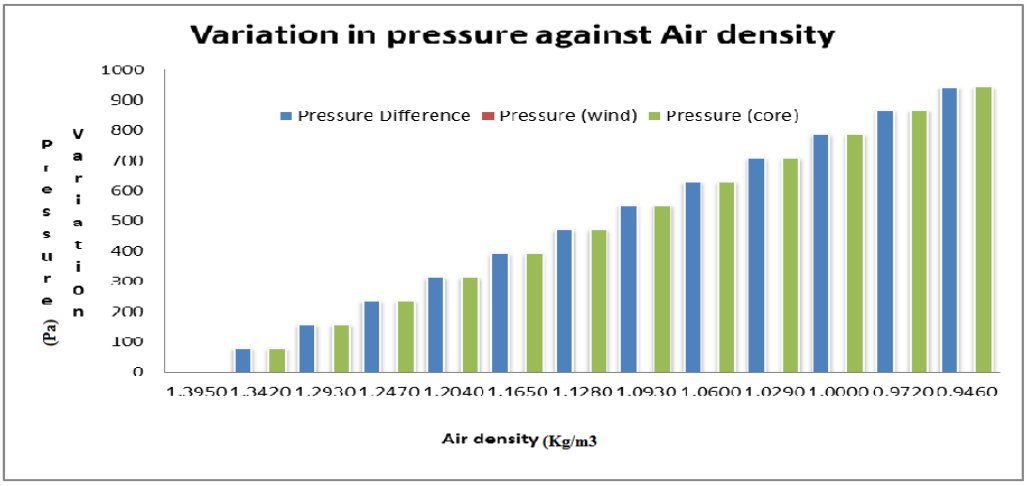

(a)

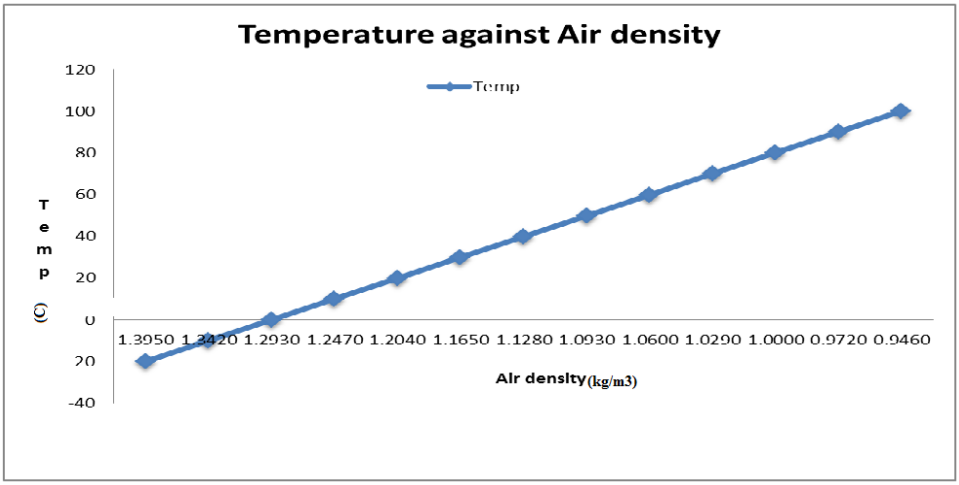

Figure 20: (a) Differential pressure varying with air density. (b) Range of ambient temperature with air density

8. The Transfer Function Characterization Simulations

The transfer function characteristics for determining the performance of the system under consideration or the response of the designed system in both time domain and in frequency domain is simulated and shown section and in subsequent subsections. This transfer function is sub-sectioned into output transfer characterization with the impedance voltage, input transfer characterization with the impedance/sensing voltage and the transfer function with the excited current.

9. The Outward Output Transfer Function with the Impedance Voltage

The response readout or the transfer function of the outward core geometry from the instrumentation electronics is given in equation 15 and 16. This characteristic obtained was simulated with the impedance voltage of equation 12. The result shows that the impedance voltage increases exponentially with substantial amount as shown in Figure 21. The outward transfer function is a ratio of the outward output voltage to the timer voltage (Impedance voltage). From Figure 21, the outward output transfer function is infinitesimal as compared to the impedance voltage. This is so because in the transfer function the effect of the excited current are cancelled since it's a ratio of two different kind of voltage. The impedance voltage is obviously higher since it a product of the excited current and the inductance characteristics.

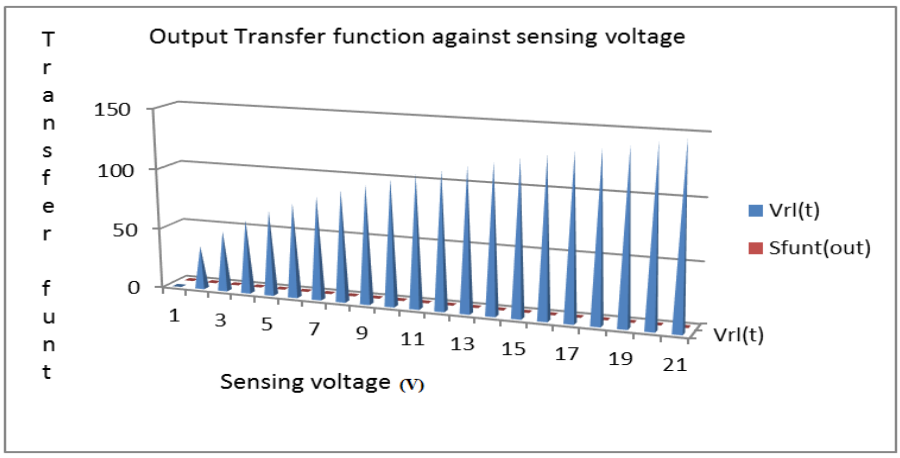

Figure 21: The effect of outward Output transfer function with the impedance voltage

10. The inward Output Transfer Function with the Impedance Voltage

The response readout or the transfer function of the inward core geometry from the instrumentation electronics is given in equation 17 and 18. The result obtained is shown in Figure 22. This shows an exponential increase in a spiral characteristic. The impedance voltage is again higher than the inward output transfer function because of the exclusion of the excited current as found in the impedance voltage that it's compared with. This is so because in the transfer function the effect of the excited current is cancelled since it's a ratio of two different kind of voltage. The impedance voltage is obviously higher since it a product of the excited current and the inductance characteristics.

The content of the transfer function characteristics is ultimately one of the contribution of this work as compared to the existing literature.

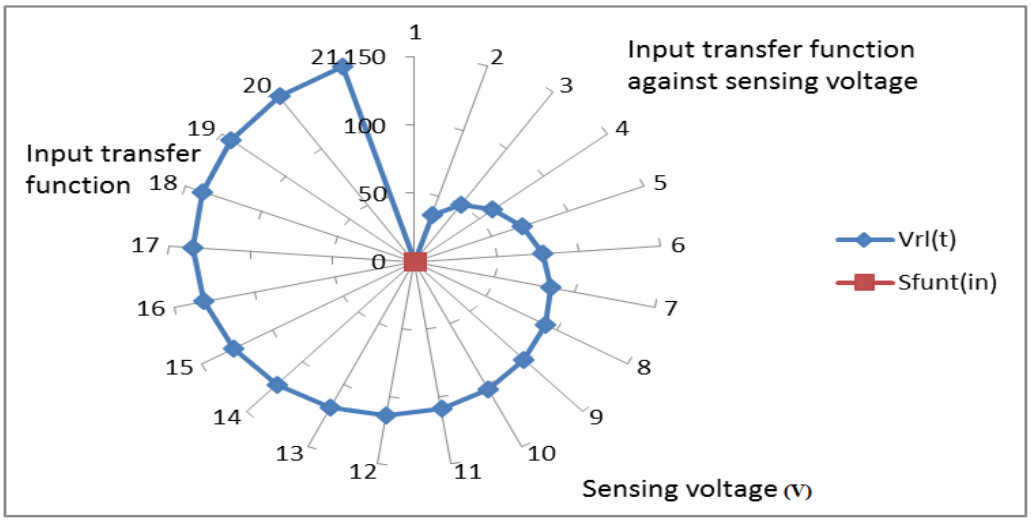

Figure 22: The effect of the inward output transfer function with the impedance voltage

11. The effect of the excitation current on Transfer Function.

The excited current causes a linear incremental path on the transfer function. This result is shown in Figure 23.

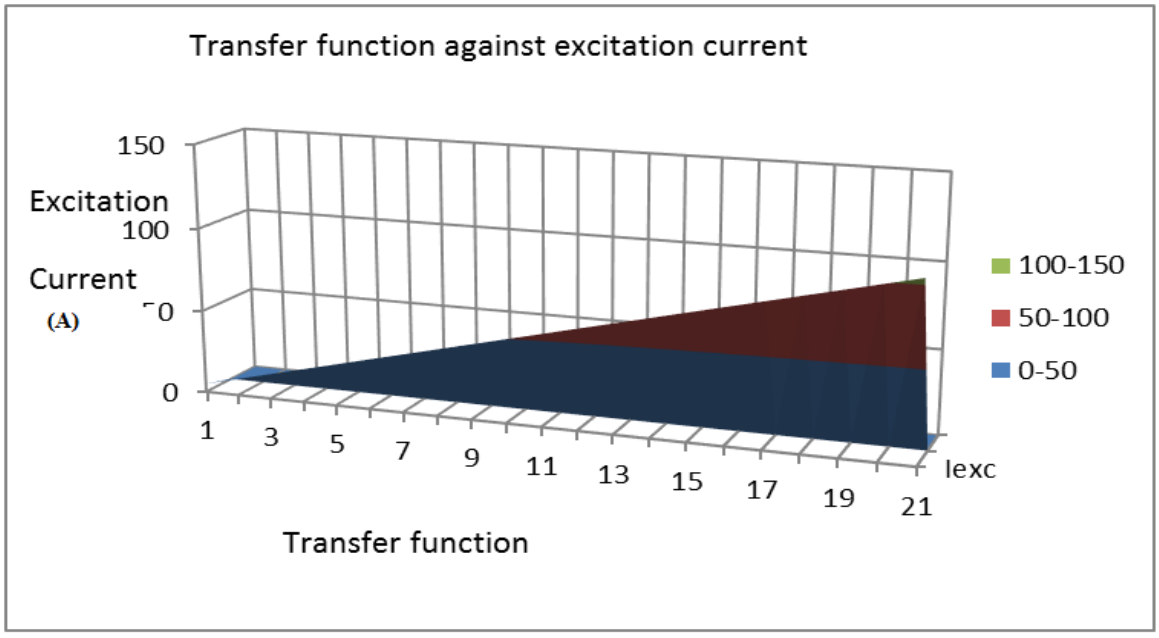

Figure 23: The effect of the excitation current on the transfer function

12. The effect of the Inward Output Voltage to Outward Output Voltage

This sub-section shows the relationship between the inward output voltage and the outward output voltage. At this junction, a correlation analysis is done. The result shows that at some point the inward output voltage increases exponentially before a linear decrease just at the point the core is about to switch over. The outward output voltage shows some increment initially then eventually decreases exponentially before attaining a linear increase. This characteristics shows some symmetrical and reciprocacity relationship in the inward and outward transduction. This is shown in Figure 24.

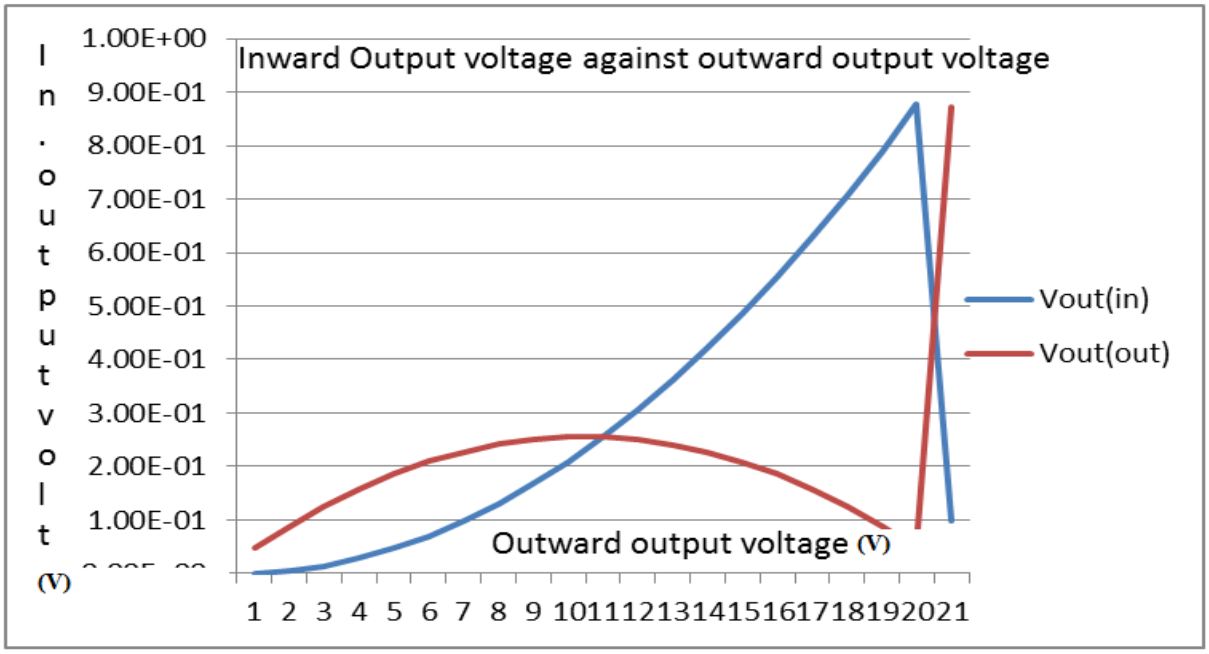

Figure 24: The effect of the inward output voltage and the outward output voltage

13. Conclusion

The transfer function of differential inductive system using seesaw oscillations and vibration has been modelled using simulation with double coil arrangement with magnetic core made of iron suspended in a seesaw. This is made to oscillate freely in order to produce the desired effect. Therefore, results such as range of convulsion bar, frequency of oscillation, frequency output, resonant frequency, magnetization and demagnetization, sweeping voltage, impedance voltage, magnetic field strength, resonant frequency, mass of bar and mass of target object and the current excitation responses are obtained, by propelling the wind force and vibrations used for the acquisition of impulsive electrical signal from a harsh environmental location and/or a machine vibration which can slowly set the seesaw into oscillation and therefore producing helpful results as characterized. The results shown can be used for characterizing the materials and hence sensor with high sensitivity, linearity and responsiveness in harsh environmental condition is obtained and characterized and their corresponding transfer functions are obtained. This help in sensing broken metallic in the body during war and sensed in hard to reach to reach locations as a result of the huge magnetic field generated. This also, verifies the derivations and the simulation in literature.

The main contribution of this research is to demonstrate the scope and potential of a circuit design of the differential sensory system, functional theory and relevant derivations on its operation details when characterizing their transfer function for signal gain. The idea is using inductive coils as transducer elements responding to changes in the parameter being sensed. This phenomenon is the result of simple

movement of a core position bringing about proportionate changes in the inductance of the circuit, and hence ultimately in the output parameters. The output parameters include frequency, duty cycle, current, voltage, frequency, frequency hysteresis, speed, acceleration, kinematics, pressure, range of oscillation, angulation, Impedance voltage, Magnetic field strength, and Transfer function.

References

1. Deji, A., Khan, S., Habaebi, H.M., Musa. O.S. (2024). Technical Engineering Evaluations and Economic Feasibility Study of Solar Powered Air Conditioning System in Tier Three Nations. *Academy of Entrepreneurship Journal,* **30(**S1): 1-18.
2. Deji A., , Sheroz K., Musse M.A., (Jan-Feb 2024). Experimentation and Application of Differential Inductive System for Machine and Human body parametric Measurement. *International Journal for Multidisciplinary Research (IJFMR).* **6**(1): 1-19. https://doi.org/10.36948/ijfmr.2024.v06i01.11787.
3. Deji A., Sheroz K., Musse M.A., (December 2023) "Analytical Modeling of Electrical Frequency and Voltage Signal from a Differential Inductive Transduction for Energy Measurement. *International Journal for Multidisciplinary Research.* **5(**6): 1-19. **DOI:** 10.36948/ijfmr.2023.v05i06.8292
4. Deji A., Sheroz K., Musse M.A., (December 2023) "Kinematic Motion Modelling from Differential Inductive Oscillation Sensing for a Sevomechanism and Electromechanical Devices and Applications. *International Journal for Multidisciplinary Research.* **5(**6: 1-15. **DOI:** 10.36948/ijfmr.2023.v05i06.8291
5. Deji A., Hanifah A.M., Sherifah O.M., (December 2023) "The Adoption of Information System Technology in Piloting the Current State of Health Institution in Tier Three Nations.*" International Journal for Multidisciplinary Research.* **5**(6): 1-13. **DOI:** 10.36948/ijfmr.2023.v05i06.8367
6. Abdulwahab D. et al., (2010). "Identification of linearized regions of non-linear transducers responses," International Conference on Computer and Communication Engineering (ICCCE'10), Kuala Lumpur, 2010, pp. 1-4, doi: 10.1109/ICCCE.2010.5556753.
7. Abdulwahab D., S. Khan, Chebil J., and Alam A. H. M. Z., (2011)."Symmetrical analysis and evaluation of Differential Resistive Sensor output with GSM/GPRS network." *4th International Conference on Mechatronics (ICOM), Kuala Lumpur, Malaysia,* pp. 1-6, doi: 10.1109/ICOM.2011.5937149.
8. Khan S., Deji A., Zahirul A.H.M., Chebil J., Shobani M.M., Noreha A.M. (Setember 2012) "Design of a Differential Sensor Circuit for Biomedical Implant Applications". *Australia. Journal of Basic and Applied. Sciences., 6(9): 1-9.* 10.1002/9781118329481.ch1.
9. Deji A., Sheroz K, Musse M.A, Jalel C. (August 2014). Analysis and evaluation of differential inductive transducers for transforming physical parameters into usable output frequency signal August 2014 *International Journal of the Physical Sciences* 9(15):339-349. DOI:10.5897/IJPS12.655
10. Deji A., Sheroz K, Musse M.A, Jalel C. (2011). Design of Differential Resistive Measuring System and its applications. *A book chapter in IIUMPRESS on Principle of Transducer Devices and Components*. Chapter 17, page 107.
11. Abdulwahab Deji (2011). Development of Differential Sensor Interface for GSM Communication. *Kulliyyah of Engineering, International Islamic University Malaysia.*
12. Abdulwahab Deji (2016). Development of Differential Inductive Transducer System for Accurate Position Measurement. *Kulliyyah of Engineering, International Islamic University Malaysia*.
13. Practical EE Copyright 2019). www.eepractical.com

14. Deji A., Sherifah OM., (2023). *The Mediating Effect of Entrepreneur Cash Waqf Intension as means of Planned Behaviour for Business Growth. International Journal for Multidisciplinary Research. 5 (6): 1-22*
15. Elfaki Ahamed, O.M.H., Musa O.S, Deji A., (2023). Factors Related to Financial Stress Among Muslim Students in Malaysia: A Case Study of Sudanese Students. Academy of Entrepreneurship Journal, 29(6), 1- 15.